



ELSEVIER



Optics Communications 6388 (2000) xxx

OPTICS
COMMUNICATIONS

www.elsevier.com/locate/optcom

Coherence-driven gain and its possible measurement in pump–probe experiments

F.B. de Jong, B.T. Wolschrijn, R.J.C. Spreeuw, H.B. van Linden van den Heuvell *

Van der Waals-Zeeman Instituut, Universiteit van Amsterdam, Valckenierstraat 65, 1018 XE Amsterdam, the Netherlands

Received 8 October 1999; accepted 18 November 1999

Abstract

We discuss the phenomenon of coherence-driven gain: the effect that oscillating atomic dipoles can amplify or attenuate a light field depending on the phase difference between dipoles and field. No inversion of atomic population is required to increase the field. This is in contrast to population-driven gain where an inverted atomic medium always contributes to gain, regardless of the phase of the light field. In particular, we discuss coherence-driven gain in two-level systems and wave-packets. We present *gedanken* experiments in an attempt to separate the phase-dependent gain from modifications of the probe pulse shape caused by the coherent pump mechanism. Experiments on electronic wave-packets in Nd:Yag are presented as an illustration. We also performed experiments using short optical pulses to excite etalon modes. These optical pulses mimic the wave-packet dynamics of matter. The experiments offer a clear interpretation of coherence-driven gain and lead to an analogy with interference on a beamsplitter and homodyne detection. © 2000 Elsevier Science B.V. All rights reserved.

PACS: 42.50.Md; 42.50.Gy; 32.80.Qk

1. Introduction

Studies on lasing without inversion (LWI) [1–4] show that LWI schemes can be generally classified in two categories: (i) schemes where a hidden inversion can be revealed, and (ii) schemes where no hidden inversion can be found and which thus seem to be “genuinely inversionless”.

In the first category the hidden inversion is revealed either in a dressed state description or through

a basis transformation of the atomic states. A dressed state type of hidden inversion is found in driven two-level atoms [5] which form the simplest medium to demonstrate lasing without population inversion. Strongly driven atoms exhibit a triplet in their fluorescence spectrum (Mollow triplet). Light can be amplified when its frequency is tuned to one of the sidebands of the Mollow triplet of strongly driven atoms [6]. This gain is independent of the phase of the probe field and can be large enough to support an oscillator; experiments showing sideband lasing have been reported in e.g. sodium [7] and in barium vapor

* Corresponding author. E-mail: heuvell@phys.uva.nl

[8,9]. While there is no population inversion in the bare states, the gain can be explained in terms of an inversion between dressed states [10]. A pump–probe detuning with the size of the Rabi frequency is required in this scheme. This sets a strong limit to the frequency up-conversion that can be obtained.

Hidden inversion revealed through a basis transformation of the atomic states requires at least a three-level system. Hidden-inversion lasing based on coherent population trapping was demonstrated in a three-level cadmium scheme [11].

In the second category “genuinely inversionless” lasing was demonstrated in rubidium [12] and sodium [13] in a three level V-scheme and Λ -scheme, respectively. The physical origin of “genuinely inversionless” lasing¹ in a three-level V-scheme has been discussed in terms of the quantum Zeno effect [15].

This paper concentrates on another form of “genuinely inversionless” lasing. When *resonant* light fields in a two-level system are applied there can be no hidden inversion in the dressed state picture. Gain, however, is still possible if the phase lag of the probe field with respect to the oscillating dipole moment formed by the two levels is between 0 and π . This gain is driven by the polarization induced through coherent pumping and does not require any inversion. Such a coherently pumped laser has been proposed [16] and recently the propagation of resonant pulses in a pump–probe experiment was discussed [17]. A special effort is made to link this subject of coherence-driven gain to other subjects where a different terminology is used but where the same physical phenomena play a role.

2. coherence-driven gain in two-level atoms

In many cases a gain medium is well approximated by a collection of two-level atoms. The atomic

dynamics are then conventionally described using a density matrix formalism, leading to the so called optical Bloch equations. We now consider an ensemble of two-level atoms. In general, these levels are embedded in a multi-level system. The influence of the other levels is incorporated in incoherent pump processes and level decay rates as indicated in Fig. 1. The λ 's denote the incoherent pumping rates from a large ground-state reservoir into the levels $|a\rangle$ and $|b\rangle$. The decay processes from these levels are indicated as γ_a and γ_b . The atomic resonance frequency is ω_0 . We write the electric field as $E(t) = \frac{1}{2}\text{Re}[\mathcal{E}_0(t)e^{-i\omega_0 t}]$, where $\mathcal{E}_0(t)$ is a complex envelope function that varies slowly compared to $e^{-i\omega_0 t}$. In the rotating-wave approximation the Bloch equations are [19]:

$$\dot{\rho}_{ab} = -\gamma\rho_{ab} + \frac{i}{\hbar}V_{ab}(t)(\rho_{aa} - \rho_{bb}) \quad (1)$$

$$\dot{\rho}_{aa} = \lambda_a - \gamma_a\rho_{aa} + \frac{2}{\hbar}\text{Im}(V_{ab}(t)\rho_{ab}^*) \quad (2)$$

$$\dot{\rho}_{bb} = \lambda_b - \gamma_b\rho_{bb} - \frac{2}{\hbar}\text{Im}(V_{ab}(t)\rho_{ab}^*) \quad (3)$$

Here $V_{ab}(t)/\hbar = -\frac{1}{2}p\mathcal{E}_0(t)/\hbar$, is the Rabi frequency, with p the component of the atomic transition dipole moment along the electric field, $\gamma = \gamma_{ab} + \gamma_{\text{ph}}$ with $\gamma_{ab} = (\gamma_a + \gamma_b)/2$ the contribution from the decay processes and γ_{ph} the contribution from the incoherent pumping and other dephasing processes.

There is gain for the field if the interaction term in Eq. (2) decreases ρ_{aa} . The gain is thus proportional to $-\text{Im}(V_{ab}\rho_{ab}^*)$. Coherence-driven gain is present if somehow a coherence ρ_{ab} has been prepared. Population inversion is not required. For example, we may prepare ρ_{ab} using a short coherent pump pulse. After a time τ we may send in a weak probe pulse with the same frequency but a different phase ϕ (see Fig. 1):

$$V_{ab}(t) = -\frac{1}{2}p\mathcal{E}_0(t) - \epsilon\frac{1}{2}p\mathcal{E}_0(t-\tau)e^{i\phi}, \quad (4)$$

(with $\epsilon \ll 1$.)

¹ A recent study [14] showed that also in the “truly inversionless” schemes a hidden inversion can be found, albeit not in a basis of atomic states but in the field reservoir.

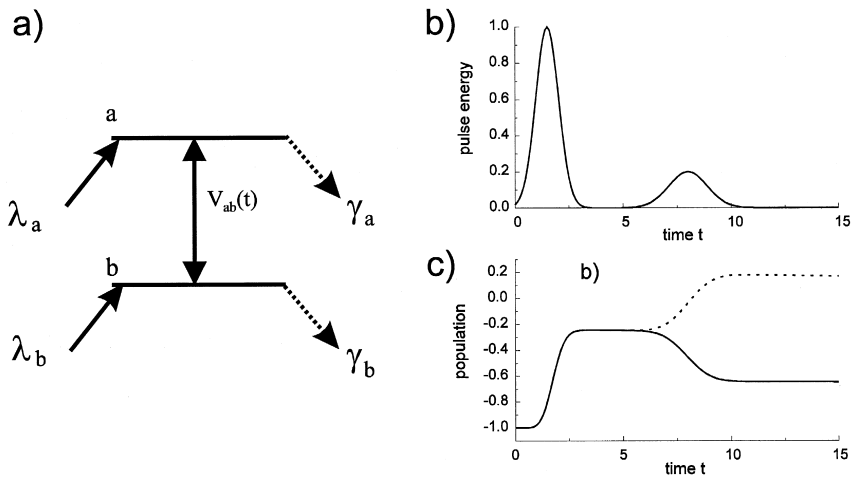


Fig. 1. (a) A two-level system embedded in a multi-level scheme. Both levels may represent excited states. (b) Sequence of pump and probe pulse. (c) Population difference $\rho_{aa} - \rho_{bb}$ as a function of time for pump–probe phase difference equal to zero (upper dotted curve, probe absorption) and π (lower solid curve, probe amplification).

The pulse durations of pump and probe and the delay τ are chosen short enough that populations and coherences are not affected by the incoherent processes during the pump–probe interaction. At $t = 0$ the coherent pump is turned on and the population starts its Rabi cycle. While ρ_{aa} is still smaller than ρ_{bb} the pump is turned off. If the probe pulse has the same phase as the pump it will lose intensity by resuming the Rabi cycle started by the pump, thus further exciting ρ_{aa} . A probe pulse with the opposite phase, however, will gain intensity by undoing the original Rabi cycle and lowering ρ_{aa} , thus extracting energy from the medium. This is coherence-driven gain: not the inversion between the levels but the phase difference between atomic dipole and probe field determines the gain. The phase difference between the dipole moment of the atom and probe field is the argument of $V_{ab} \rho_{ab}^*$.

If the pumping process is *incoherent*, in such a way that there is population inversion and $\rho_{ab} = 0$, the probe will experience gain regardless of the phase ϕ . In Eq. (1) $V_{ab}(t)$ couples to the population difference to generate a non-zero ρ_{ab} . This yields ‘regular’ *inversion-driven* gain. For negative inversion, $\rho_{aa} - \rho_{bb} < 0$, the phase of ρ_{ab} is opposite, leading to attenuation instead of gain.

The distinction between the two gain mechanisms can be summarized as follows. *Coherence-driven gain* occurs when the probe couples directly to the atomic dipole as created by the pumping mechanism, and is phase dependent. *Population-driven gain* occurs when the probe couples to a positive inversion, creating a dipole moment to which it can couple for gain. There is no phase dependence.

3. Stepwise reduction of coherence-driven gain to a parametric process

3.1. Dilemma in defining probe gain

The Bloch equations (1)–(3) describe how atoms respond to a light field, not how the light field responds to the atoms. In reality the atom field interactions form a coupled system. Is the concept of separate pump and probe pulses applicable in this case? In an ideal situation the pump pulse modifies the medium and a later probe pulse probes these modifications, including the evolution after the modification. In practice, the pump pulse is reshaped. If

the pump pulse is short, its spectrum is necessarily wide. The absorption of spectral components makes the pump pulse longer. The narrower the absorption features are, the longer the pump pulse is extended. Therefore the pump pulse may not be extinguished when the probe pulse arrives. In that case pump and probe pulse overlap after passing the medium, which makes it difficult to define the probe gain. The two pulses can be distinguished if they propagate in a slightly different direction. However, the phase difference can be well-defined only when the pulses are parallel. When the angle between the two beams is larger than the diffraction limit, the variation of phase differences is larger than 2π .

One may also try to separate the pulses in time and ask how large the time difference should be, in order to discriminate between pump and probe. The time separation should then be at least the lifetime of the excited states of the atoms. This answer is disturbing because in this case the probe pulse is too late to probe anything at all that could have been caused by the pump pulse. All atoms have decayed by spontaneous emission before the probe pulse arrives.

3.2. Dephasing and rephasing of a photon echo

The requirement that the probe delay should be at least the lifetime of the excited states, $\tau \ll T_1$, can be relaxed to the free induction decay time, $\tau \ll T_2$. If $T_2 \ll T_1$ the excited states are still populated after the free induction decay. However the dipole moments of individual atoms no longer add up to a macroscopic dipole and so coherent light is no longer emitted.

If this were the final situation, there would be no polarization for the probe to interact with. Therefore the probe could not be amplified. However, there is a well-known technique to repair the phase scrambling, namely by means of a so-called photon echo. A π -pulse is applied following the initial pump pulse after a delay time τ , with $T_2 < \tau < T_1$. This π pulse reverses the dephasing of the individual dipoles so that after a delay 2τ the dipoles are again in phase. This restored macroscopic dipole moment can amplify the probe pulse, if the phase difference between probe and dipole is correct. However, due to the

restored dipole moment a photon echo is emitted, overlapping in time with the probe pulse. The echo should be considered as part of the reshaped pump pulses, so that again it is difficult to the pump and the probe.

3.3. Dephasing and periodic rephasing in a wave packet

Periodic dephasing and rephasing is a well-known phenomenon in wave-packet dynamics. When the atomic upper state has a structure of regularly spaced absorption lines, a coherent superposition of excited states is known as an electronic wave packet. Excitation of such a wave packet leads to similar phenomena as sketched before. Two neighboring levels with energy difference ΔE acquire a phase difference $\Delta\phi = \Delta E t / \hbar$ after time t . This leads to complete phase scrambling on a timescale $t_{\text{scr}} = 2\pi / \Delta\Omega$, with $\Delta\Omega$ the overall frequency width of the excited-state manifold, see the bell shaped line in Fig. 2(a). However, if the energy spacings are approximately equidistant it is possible to wait until all phase differences between neighbors are approximately 2π . The time at which this occurs is usually called the orbiting time of the wave packet and is long compared to t_{scr} , the dephasing time of the macroscopic dipole moment. It can also be short compared to the population decay time T_1 . After a delay of the orbiting time it is possible to amplify a probe pulse. Experiments demonstrating this rephasing and its effect on the probe propagation are described in Section 4.

The phase-sensitive probing of a wave packet as a possibility of lasing without inversion, has an all-optical analogue. We can replace the electronic eigenstates of an atom by the modes of a Fabry–Perot etalon. We then couple a short light pulse into the etalon (exciting a coherent superposition of longitudinal modes). The wave packet is simply a pulse of light bouncing back and forth between the mirrors. Obviously the bandwidth of the pump pulse should be large compared to the free spectral range of the etalon, see Fig. 2(b) and Fig. 2(c). A well-timed and well-phased probe pulse can be amplified with the help of the light stored in the etalon. The optical pulse that has completed one round trip inside the

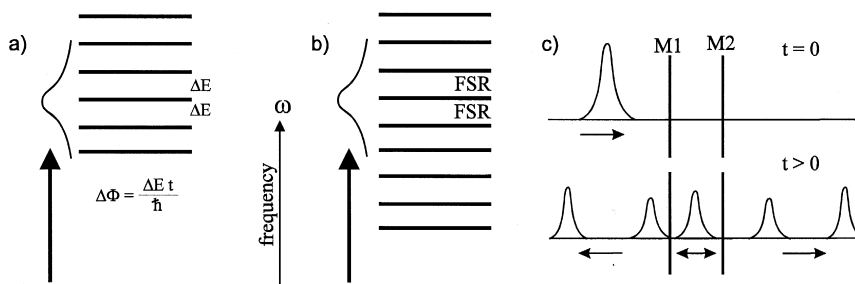


Fig. 2. (a) Wave packet excitation; a set of closely spaced energy levels excited simultaneously by a broadband pulse. (b) Etalon excitation, several longitudinal modes are excited by a broadband pulse. (c) Short pulse excitation of the etalon in the time domain. The etalon mirrors are indicated with M1 and M2. The pulse duration is shorter than the round-trip time in the etalon. The etalon shows ringing in analogy to the wave-packet recurrences.

etalon can interfere constructively with the probe pulse. The probe pulse then reflects off the input mirror with a reflectivity larger than one, extracting energy from the optical cavity.

At this point we have reduced the medium of our coherence-driven laser without inversion, down to the situation where no *atomic* medium is left.

3.4. Interference on a beamsplitter

In our example of an optical wave packet, what was initially introduced as amplification is now found to be simply interference of waves. Even the etalon can be eliminated. The essential process takes place at the input mirror of the etalon. Having noticed that various coherent processes show ‘lasing without inversion’ (we sketched phase-sensitive probing of a wave packet and photon echo generation as examples), we finally add interference of two fields at a beamsplitter, yielding two beams with amplitudes given by the sum and the difference of the amplitudes of the incoming beams. Etalons and beamsplitters are passive and linear devices. Nevertheless a signal (e.g. present in the form of modulation of the carrier of the probe pulse) can be amplified. This reduced version of ‘coherence-driven gain’ that we have presented is in fact applied in homodyne detection.

In the subsequent sections the above-described gedanken experiments involving wave packets, both

in an atomic medium and in a Fabry–Perot etalon, are actually performed and described.

4. Wave-packet experiments

4.1. Introduction

In a typical wave-packet experiment a broad-band laser excites a superposition of closely spaced excited states, for instance atomic Rydberg states [20] or molecular rovibrational states [21]. The wave-packet evolution is probed by a second pulse that ionizes the atom or molecule. The second, ionizing, pulse is a probe for the position of the wave-packet.

The laser light is in principle also affected by the wave packet dynamics. For example, excitation of a wave packet leads to absorption. A wave-packet recurrence can lead to a field increase at a later time. Until recently [18] wave-packet dynamics has been measured through the atoms or molecules; changes in the light intensities were too small to be detected. The experiments in this section show that wave-packet dynamics can be measured in the intensity of pump and probe light.

To achieve a measurable amount of absorption we have chosen a dense atomic medium, Nd^{3+} ions in a host crystal of Yttrium Aluminum Garnet (Nd:yag). The absorption is varied using different lengths of Nd:yag rods, ranging from 2 mm to 12 cm. The

ground state of the Nd^{3+} ion is the lowest level in the $^4I_{9/2}$ manifold. We drive transitions from the ground state to the $^4F_{5/2}$ manifold. The degeneracy in magnetic quantum number M_J is lifted in the crystal field. Due to the tetragonal symmetry of the crystal field there are $J + \frac{1}{2}$ Stark levels [22]. With a short laser pulse we excite a superposition of these Stark levels. This coherent superposition describes the precession of the angular momentum of the Nd^{3+} -ion in the crystal field.

Transitions from the ground state to the $^4F_{5/2}$ manifold have wavelengths at about 820 nm, well within the tuning range of a Ti:Sapphire laser. The lines in the manifold have a large inhomogeneous broadening due to variation of the ion positions in the crystal field. The absorption spectrum of this manifold is given in Fig. 3(a). The spectrum of the exciting laser pulse is Gaussian with a bandwidth of 125 cm^{-1} centered around 12260 cm^{-1} . In the inset of Fig. 3(b) the product of the neodymium absorption spectrum with this Gaussian pulse is plotted. From this frequency spectrum we can calculate the time evolution of the wave packet using Fourier transformation. Fig. 3(b) shows the Fourier transform, assuming a Fourier limited (i.e. unchirped) pulse. We recognize wave-packet recurrences around 0.5 ps, 1 ps and 1.5 ps, resulting from the energy difference of the almost equidistant transitions of neodymium in this interval (65 cm^{-1}). Only a few

recurrences appear, showing that the wave packet dephases very rapidly. This is a result of the large inhomogeneous broadening of the individual spectral lines.

4.2. Experimental set-up

A schematic drawing of the set-up is given in Fig. 4. We use a mode-locked Ti:Sapphire laser which produces pulses of 150 fs at a repetition rate of 72.5 MHz. The pulses have a bandwidth of 125 cm^{-1} and a pulse duration of 150 fs so are close to Fourier limited (a factor 1.3 larger than the limit for Gaussian pulses). The beamsplitter in the Michelson interferometer splits the laser pulse in a pump pulse and a probe pulse, with comparable intensities. Using a delay line the timing of the probe pulse can be varied over several picoseconds.

To measure the wave-packet dynamics we use a phase-sensitive pump–probe technique [23], which measures the overlap of the excited wavefunction after a certain delay with the initially excited wavefunction. A glass plate wiggler oscillating at 12 Hz is put in one arm of the interferometer. This wiggler introduces an oscillating path-length difference of many wavelengths, resulting in an optical phase modulation at 8 kHz. The pump and probe pulse interfere on the photomultiplier. The part of the signal that is

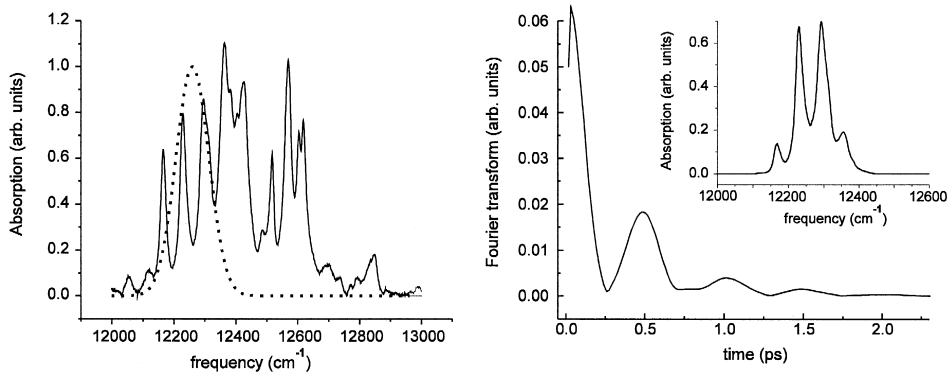


Fig. 3. (a) The absorption spectrum of Nd:YAG at room temperature, solid line. The dotted line gives the frequency spectrum of a Gaussian pulse with a central frequency of 12260 cm^{-1} and a bandwidth of 125 cm^{-1} . The product of the Gaussian pulse shape and the Nd:YAG spectrum is given in the inset of (b). The calculated Fourier transform is depicted in Fig. (b). This curve represents the time evolution of the wave packet, formed by the coherent superposition of the absorbing states.

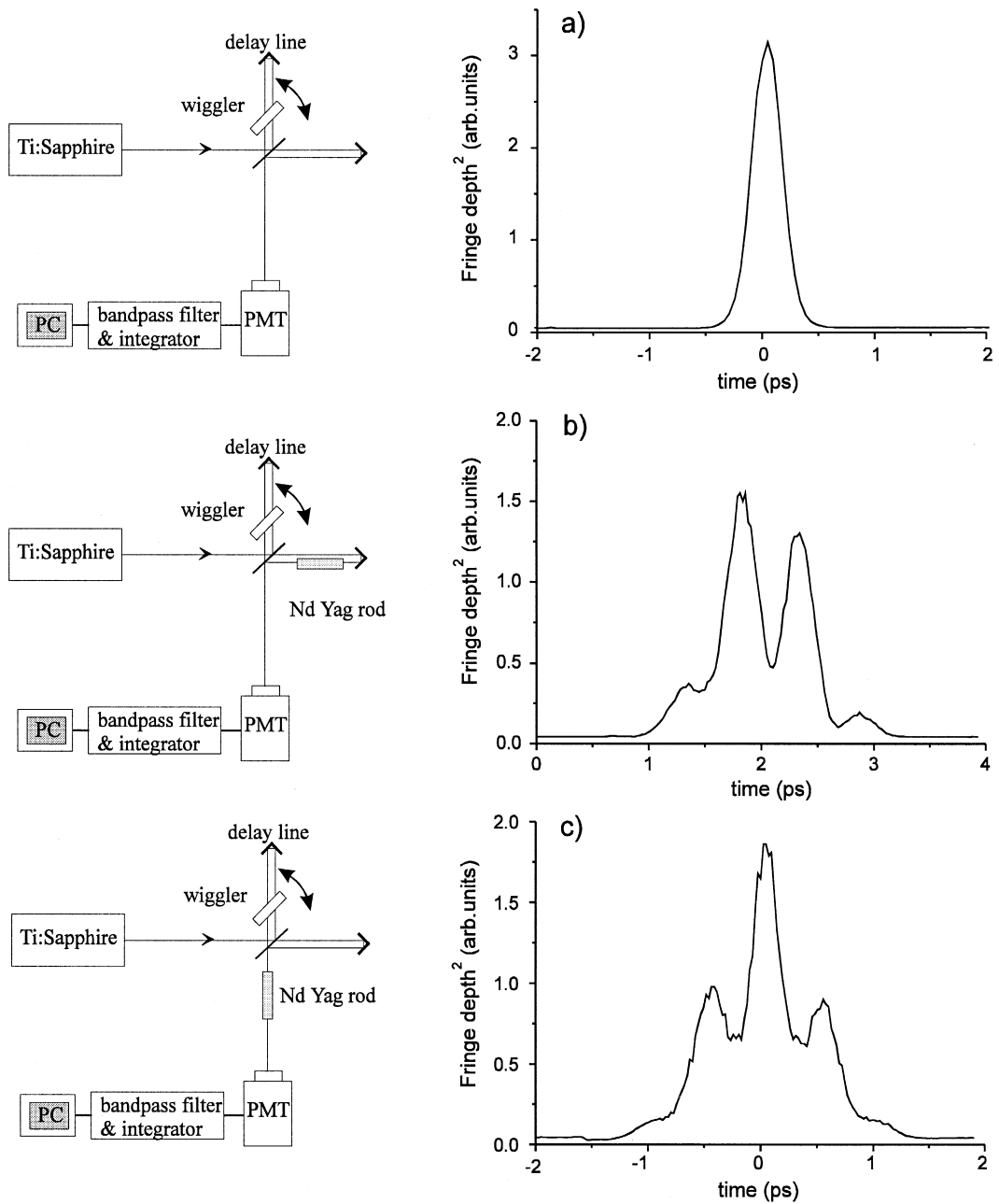


Fig. 4. The experimental set-up for measuring wave-packet dynamics in the Nd:yag crystal. (a) Result without Nd:yag crystal, the field-correlate of the pulse. (b) Nd:yag crystal is put in one arm of the interferometer. (c) The Nd:yag crystal is placed after the interferometer. The set-up pictures on the left correspond with the experimental results on the right side.

modulated by the wiggler is extracted by a 8 kHz bandpass filter. The filtered signal is squared and averaged. This gives the squared fringe depth.

The values are stored in a personal computer as a function of the pump–probe delay time. The total integration time for each step of the delay line is

about 5 s. After each fringe measurement a step of 15 μm (50 fs) is made. The advantage of the wiggler technique is that it does not require an interferometrically stable set-up.

The relation between the observed signal and the population amplitude of the excited levels in the notation of Ref. [24] is as follows. The excited wave function after pump and probe pulse is

$$|\Psi_{\text{total}}\rangle = |\Psi(\tau)\rangle + |\Psi(0)\rangle. \quad (5)$$

Both wavefunctions can be decomposed in their eigenstates,

$$\Psi(\tau) = \sum_n a_n e^{-i\omega_n\tau} |n\rangle. \quad (6)$$

The total excited-state wave function is

$$|\Psi_{\text{total}}(\tau)\rangle = \sum_n a_n (1 + e^{-i\omega_n\tau}) |n\rangle, \quad (7)$$

and the excited population is

$$\begin{aligned} P(\tau) &= \langle \Psi_{\text{total}}(\tau) | \Psi_{\text{total}}(\tau) \rangle \\ &= \sum_n 2|a_n|^2 (1 + \cos(\omega_n\tau)). \end{aligned} \quad (8)$$

with a constant part $\sum_n 2|a_n|^2$ and an oscillating part $\sum_n 2|a_n|^2 \cos(\omega_n\tau)$. The observed signal is the square of the oscillating part, time averaged by the wiggler over $2\Delta\tau$ around the delay time τ

$$I = \int_{\tau-\Delta\tau}^{\tau+\Delta\tau} \left(\sum_n 2|a_n|^2 \cos(\omega_n\tau') \right)^2 d\tau'. \quad (9)$$

This integral has an appreciable value only when all the cosines add up in phase. This is the case when the evolving wavepacket has overlap with its initial shape, i.e. when τ is a multiple of the orbiting time $\hbar/(\omega_{n+1} - \omega_n)$.

The result of a pump–probe scan without Nd:yag rod, as a function of pump–probe delay time is given in Fig. 4(a). This shows the squared autocorrelate of the field. The full-width-at-half-maximum (FWHM) measures the coherence length of the pulse and not the actual pulse duration.

4.3. Measuring wave-packet dynamics in a pump–probe experiment

In order to measure the wave-packet dynamics as predicted on the basis of the absorption (given in

Fig. 3), we introduce an 8-cm long Nd:yag rod in the fixed arm of the Michelson interferometer, see Fig. 4(b). The alignment is such that the pump pulse passes the Nd:yag crystal only once. We have increased the probe delay by 130 ps, to compensate for the additional delay of the pump pulse due to traveling a distance of 8 cm through a medium with refractive index 1.5. The probe pulse is scanned over several picoseconds to measure the interference fringes with the pump light. In this set-up the probe measures the modification of the pump pulse after passing the medium. Fig. 4(b) shows that the pump pulse is stretched out to a length of about 2 ps. There are two wave-packet recurrences, at $t = 2.5$ ps and $t = 3$ ps. This optically detected wave packet recurrence time of 0.5 ps is consistent with the time based on the spectral information from absorption, see Fig. 3.

When the Nd:yag rod is placed after the Michelson interferometer as indicated in Fig. 4(c), both pump and probe pulse pass the crystal. The wave-packet recurrences induced by the pump pulse now overlap with the probe pulse. The wave-packet from the pump pulse interferes with the wave packet from the probe pulse, or equivalently, the modified probe pulse interferes with the modified pump pulse.

Since the probe is scanned in delay time by the wiggler, there is no fixed phase relationship between pump field and probe field. The signal in Fig. 4(c) is an average over both constructively and destructively interfering wave packets. This is inherent to the method of measurement as described above. In the following section we change the set-up to keep a fixed phase relation between pump and probe pulse, enabling us to investigate the constructive or destructive interference separately.

4.4. Measuring coherence-driven gain in a pump–probe experiment

The wave packet excited by the pump pulse can only interact again with the optical field after one recurrence time. If the probe pulse is timed such that it arrives after one recurrence time, the wave packet that it creates interferes constructively or destructively with the recurring wave-packet from the pump. This depends on the phase difference $\Delta\Phi$ between

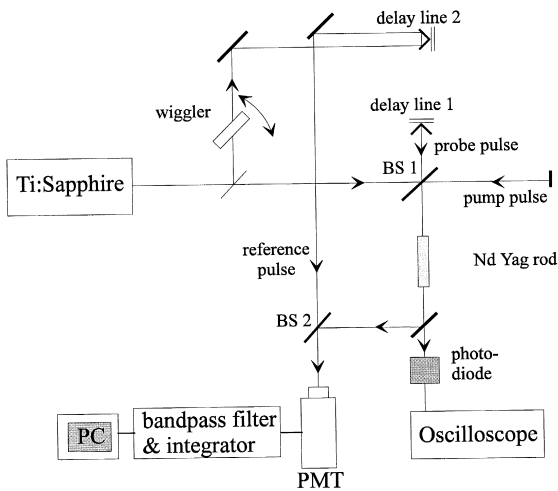


Fig. 5. Experimental set-up for measuring coherence-driven gain. Pump and probe pulse pass through the Nd:Yag sample and are compared with the reference pulse. BS 1 and BS 2 indicate the beamsplitters in the Michelson interferometer and the beamsplitter that combines the three pulses, respectively.

the probe field and the dipole moment formed by the ground state and wave-packet. By constructive wave-packet interference we mean that the probe light is absorbed to add to the wave-packet amplitude. Destructive interference means that the wave-packet is destroyed and its energy added to the probe

field by stimulated emission. Thus constructive wave packet interference implies destructive interference for the field amplitudes and vice versa.

In order to measure these effects the set-up is modified as depicted in Fig. 5. Delay line 2 is added to provide a second probe pulse which serves as an unperturbed reference. This second probe beam (reference pulse) is scanned over several picoseconds and probes the combined pump and probe field. The reference pulse is combined with the pump–probe beam at the second beamsplitter, BS 2. The fringes are measured in same way as in the previous two-pulse experiments.

We fix delay line 1 to give a pump–probe delay equal to one recurrence time (0.5 ps). This delay line is interferometrically stable. The precise delay is actively controlled to keep a constant phase difference. The photodiode after the Nd:Yag rod (see Fig. 5) measures the pump–probe interference fringes. The signal is kept maximal or minimal by adjusting the voltage on a piezo electric element in the mirror mount.

Fig. 6(a) shows the pump and probe pulse after passing the Nd:Yag rod separately. Pump and probe pulse differ only in timing and amplitude. Note that the delay in the probe pulse matches one recurrence time.

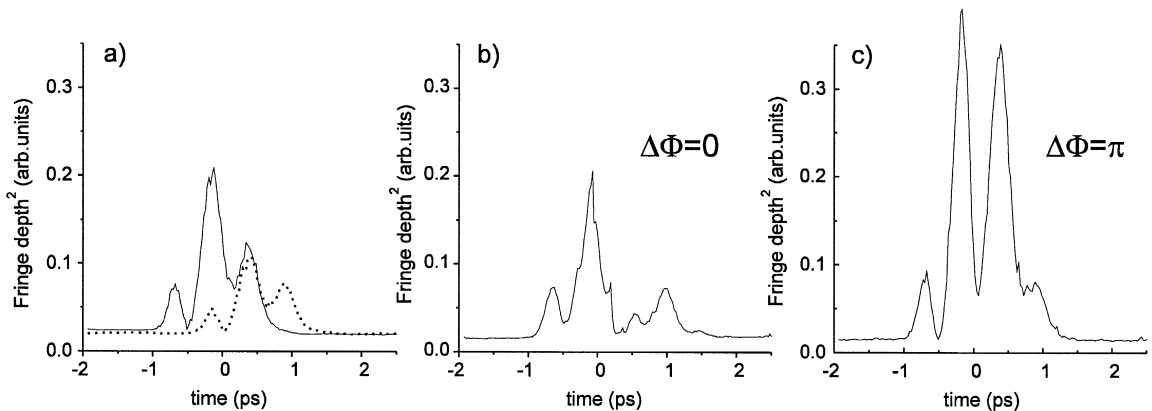


Fig. 6. The time structure of pump and probe pulse after passing the Nd:Yag crystal. The probe pulse is delayed by one recurrence time of 0.5 ps using delay line 1. After passing the Nd:Yag crystal the pump and probe pulse are compared with the reference pulse which is delayed by delay line 2. The reference pulse is scanned in delay time over 4.5 ps. (a) The pump pulse (solid line) and probe pulse (dotted line) measured one without the other. (b) Both pump and probe pulse pass the Nd:Yag crystal, their phase difference is 0. (c) The same but now the pump–probe phase difference is π .

The next step is the actual three-pulse experiment in which both pump and probe pass the Nd:Yag crystal. The results for pump–probe phase difference $\Delta\Phi = 0$ and π are given in Fig. 6(b) and Fig. 6(c).

We would *like* to interpret these results as follows. The pump pulse arrives at $t = 0$ ps. At $t = 0.5$ ps we recognize in Fig. 6(a) contributions from the probe pulse and a recurrence of the pump pulse. When $\Delta\Phi = \pi$ the probe pulse creates a wave packet that destroys the wave packet created by the pump pulse. The released energy is added to the probe field in the form of stimulated emission, as can be seen in the high peak at $t = 0.5$ ps in Fig. 6(c). This is coherence-driven gain. Energy deposited in the medium by the pump pulse, is extracted by the probe pulse. [Evidently for $\Delta\Phi = 0$ the probe pulse is absorbed, as indicated by the small peak at $t = 0.5$ ps in Fig. 6(b)].

However, this interpretation can be criticized as follows. It is not possible to distinguish the interference of the wave-packet contributions in the Nd:Yag rod from interference of modified pump and probe pulses at the photomultiplier. In fact, identical results were obtained when we moved the Nd:Yag rod before the beamsplitter BS 1. The result is the correlation function of the deformed pulse. In that case only one pulse passes through the rod. The transmitted, modified pulse is then split and made to interfere with itself with a time delay.

5. Optical wave packets in a Fabry–Perot etalon

Instead of coherently exciting closely spaced levels in atoms or molecules, we can also excite various longitudinal modes in a Fabry–Perot etalon [25]. Using short pulses from a Ti:Sapphire laser to excite several etalon modes we obtain an analogy to the electronic wave-packet dynamics, see Fig. 2. Since there is no atomic medium involved, the interpretation of these experiments is more simple.

In the set-up of Fig. 5 we have replaced the Nd:Yag rod by a 2 mm quartz etalon. The mode spacing (Free Spectral Range) of this etalon (1.7 cm^{-1}) is much smaller than the bandwidth of the Ti:Sapphire laser (125 cm^{-1}) which enables us to

excite many modes coherently. Since the Ti:Sapphire pulses are almost Fourier limited the equivalent statement in the time domain is that the laser pulses (150 fs) are much shorter than the round-trip time in the etalon (20 ps).

Just like there are recurrences in wave-packet dynamics the etalon shows ringing. A pulse of light travels back and forth in the etalon while slowly leaking out at the reflecting surfaces. After exciting a wave-packet there is no interaction with the optical field possible until the recurrence time. The analog etalon statement is that only when the bouncing pulse has returned to the reflecting surface, it can interact with a probe pulse.

By using short pulses to excite an etalon we demonstrate coherence-driven gain, similar to the wave-packet experiments from the previous section. After excitation with a pump pulse, energy is stored in the etalon. This energy is ringing out on both sides of the etalon. A probe pulse with the right phase and delay time can interfere destructively with the first pulse that is bouncing back and forth. The ringing is then stopped and the energy is transferred to the probe pulse, which reflects off the input mirror with a reflectivity larger than one.

We have measured the pump–probe dynamics both in transmission and reflection (Fig. 7), using the same technique as in the previous section. The exponential decay of the pump-pulse ringing [Fig. 7(a)] is indicated with a dotted line. Fig. 7(b) and 7(c) show the effect of a probe pulse with a 20 ps delay and a phase difference 0 and π , respectively. Clearly the probe pulse can either enhance or destroy the ringing of the etalon, thereby losing or gaining energy.

We have also measured the back reflected pump and probe pulse. Since the direct back reflection of the pump pulse is too strong, we have plotted the results starting from $t = 20$ ps. The signal at $t = 0$ ps and $t = 20$ ps is shown in the inserts. Fig. 7(d) shows the ringing of just the pump pulse in the backward direction. The back reflected pump pulse arrives at $t = 0$ ps. Fig. 7(f) shows how the ringing of the etalon is stopped by the probe pulse which arrives after 20 ps with a π phase difference. The insert shows that the etalon energy is added to the probe pulse which is amplified. In Fig. 7(e) the pump–probe phase difference is 0 and the amplitude of the etalon ringing is increased.

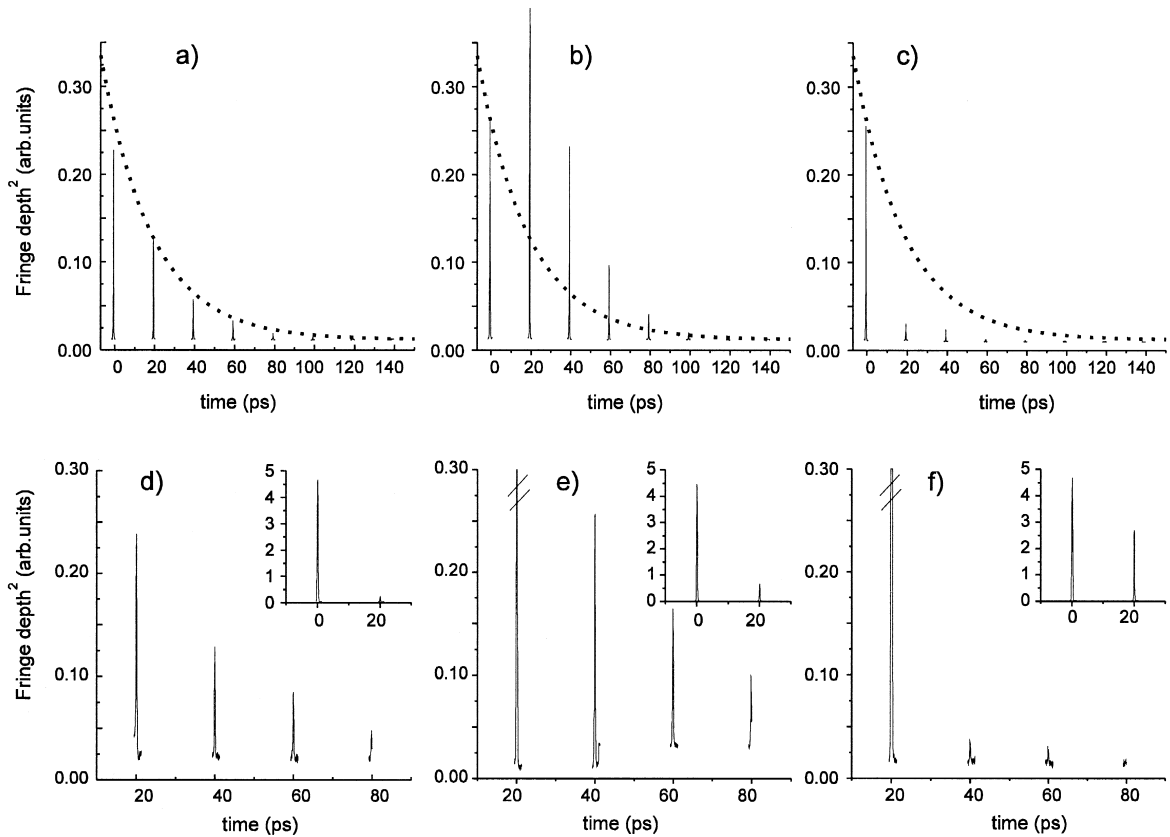


Fig. 7. Upper three graphs: etalon measurements in the forward direction (transmission). (a) The pulse train generated by the pump pulse and its decay rate. (b) The pulse train leaving the etalon in a pump–probe experiment. The phase difference $\Delta\Phi$ equals zero, therefore the pulse train is amplified. (c) The same but now the phase difference $\Delta\Phi$ is π , therefore the pulse train vanishes. The lower three graphs show etalon measurements in backward direction (reflection). The pump pulse arrives at $t = 0$ ps, the probe pulse at $t = 20$ ps. The back reflected pump and probe pulse are given in the insets. (d) The ‘normal’ recurrences of the pump if there is no probe. (e) $\Delta\Phi = 0$, the probe enlarges the recurrences. (f) $\Delta\Phi = \pi$, the probe empties the cavity at once and no recurrences are left. The inset shows that the back reflected probe is amplified.

Since these etalon experiments involve no atomic medium, there can be no discussion as to what the physical process behind the attenuation or amplification of the probe pulse is. It is obviously interference of the field amplitudes at the reflecting surfaces of the etalon. The basic process of interference takes place at *one* of the etalon mirrors, therefore a beamsplitter could just as well serve as medium to observe ‘coherence-driven gain’. By combining an information carrying beam (e.g. AM modulation) and a constant beam with the right phase on a beamsplitter, the amplitude of the modulation grows proportional with the energy of the constant beam. This ‘coherence-driven gain’ is in fact well known as homo-

dine detection, with the constant beam as the local oscillator.

6. Conclusion

We have discussed the concept of ‘coherence-driven gain’ (as opposed to gain driven by population inversion) and demonstrated it in several systems. We have shown phase-sensitive coherence effects in wave-packet experiments, showing that the wave-packet dynamics can be measured in the modification of the light pulses that are used to excite the wave packet. In analogy with the wave-packet exper-

iment, we have excited longitudinal modes in an etalon. After exciting the etalon with a pump pulse, the probe pulse could be either attenuated or amplified depending on the phase of the probe pulse.

We have discussed attempts to separate gain on the probe beam from interference of probe and reshaped pump pulse. This led us to seek a situation where pump-induced polarization quickly decays but revives later to interact with the probe. However, a revival of the polarization (dipole moment) implies that the medium is emitting energy from the pump. Therefore we conclude that in all cases studied, the probe gain is identical with constructive interference between (reshaped) probe and reshaped pump.

This is demonstrated most dramatically in the last example of an optical pulse bouncing back and forth in a Fabry–Perot etalon. The simplest example of coherence-driven gain is therefore plain constructive interference on a beamsplitter, in particular situations known as homodyne detection.

Acknowledgements

We like to acknowledge stimulating discussion with H.G. Muller. This work is part of the research program of the ‘‘Stichting voor Fundamenteel Onderzoek van de Materie’’ (Foundation for the Fundamental Research on Matter) and was made possible by financial support from the ‘‘Nederlandse Organisatie voor Wetenschappelijk Onderzoek’’ (Netherlands Organization for the Advancement of Research). The research of R.S. has been made possible by financial support from the Royal Netherlands Academy of Arts and Sciences.

References

- [1] O.A. Kocharovskaya, Phys. Rep. 219 (1992) 175.
- [2] M.O. Scully, Phys. Rep. 219 (1992) 191.
- [3] P. Mandel, Contemp. Phys. 34 (1993) 235.
- [4] E. Arimondo, in: E. Wolf (Ed.) Progress in Optics, North-Holland, Amsterdam, 1996, Vol. XXXV, Chap. V, pp. 258–354.
- [5] L. Allen, J.H. Eberly, Optical resonance and two-level atoms, General Publ. Comp. Ontario, 1987.
- [6] F.Y. Wu, S. Ezekiel, M. Ducloy, B.R. Mollow, Phys. Rev. Lett. 38 (1977) 1077.
- [7] D. Grandclément, G. Grynberg, M. Pinard, Phys. Rev. Lett. 59 (1987) 40.
- [8] A. Lezama, Y. Zhu, M. Kamskar, T.W. Mossberg, Phys. Rev. A. 41 (1990) 1576.
- [9] Q. Wu, D.J. Gauthier, T.W. Mossberg, Phys. Rev. A. 49 (1994) R1519.
- [10] P.L. Knight, P.W. Milonni, Phys. Rep. 66 (1980) 21.
- [11] F.B. de Jong, A. Mavromanolakis, R.J.C. Spreeuw, H.B. van Linden van den Heuvell, Phys. Rev. A 57 (1998) 4869.
- [12] A.S. Zibrov, M.D. Lukin, D.E. Nikonov, L.W. Hollberg, M.O. Scully, V.L. Velichansky, H.G. Robinson, Phys. Rev. Lett. 75 (1995) 1499.
- [13] G.G. Padmabandu, G.R. Welch, I.N. Shubin, E.S. Fry, D.E. Nikonov, M.D. Lukin, M.O. Scully, Phys. Rev. Lett. 76 (1996) 2053.
- [14] O. Kocharovskaya, Y.V. Rostovtsev, A. Imamoglu, Phys. Rev. A 58 (1998) 649.
- [15] F.B. de Jong, R.J.C. Spreeuw, H.B. van Linden van den Heuvell, Phys. Rev. A 55 (1997) 3918.
- [16] N. Lu, Opt. Commun. 73 (1989) 479.
- [17] J. Czub, J. Fiutak, W. Miklaszewski, Opt. Commun. 147 (1998) 61.
- [18] J. Arlt, C. Weiss, G. Torosyan, R. Beigang, Phys. Rev. Lett. 79 (1997) 4774.
- [19] P. Meystre, M. Sargent III, Elements of Quantum Optics, Springer-Verlag, Berlin, 1990.
- [20] J. Wals, H.H. Fielding, J.F. Christian, L.C. Snoek, W.J. van der Zande, H.B. van Linden van den Heuvell, Phys. Rev. Lett. 72 (1994) 3783.
- [21] N.F. Scherer, R.J. Matro, M. Du, A.J. Ruggiero, V. Romero-Rochin, J.A. Cina, G.R. Fleming, S.A. Rice, J. Chem. Phys. 95 (1991) 1487.
- [22] J.A. Koningstein, J.E. Geusic, Phys. Rev. 136 (1964) A711.
- [23] J.F. Christian, B. Broers, J.H. Hoogenraad, W.J. van der Zande, L.D. Noordam, Opt. Commun. 103 (1993) 79.
- [24] L.C. Snoek, A study of intramolecular dynamics using time-resolved spectroscopy and electron-ion coincidence techniques Ph.D. thesis, University of Amsterdam (1997).
- [25] L.D. Noordam, B. Broers, A. ten Wolde, H.G. Muller, A. Lagendijk, T.F. Gallagher, H.B. van Linden van den Heuvell, Physica B 175 (1991) 139.